

# Critical behavior in earthquake energy dissipation

James Wanliss<sup>1</sup>, Víctor Muñoz<sup>2</sup>, Denisse Pastén<sup>2,3,a</sup>, Benjamín Toledo<sup>2</sup>, and Juan Alejandro Valdivia<sup>2,4</sup>

<sup>1</sup> Department of Physics and Computer Science, Presbyterian College, Clinton, South Carolina, USA

<sup>2</sup> Departamento de Física, Universidad de Chile, 3425 Las Palmeras, Ñuñoa, Santiago, Chile

<sup>3</sup> Advanced Mining Technology Center, Universidad de Chile, Santiago, Chile

<sup>4</sup> Centro para la Nanociencia y la Nanotecnología, CEDENNA, Santiago, Chile

Received 4 November 2016 / Received in final form 21 March 2017

Published online 6 September 2017 – © EDP Sciences, Società Italiana di Fisica, Springer-Verlag 2017

**Abstract.** We explore bursty multiscale energy dissipation from earthquakes flanked by latitudes  $29^\circ$  S and  $35.5^\circ$  S, and longitudes  $69.501^\circ$  W and  $73.944^\circ$  W (in the Chilean central zone). Our work compares the predictions of a theory of nonequilibrium phase transitions with nonstandard statistical signatures of earthquake complex scaling behaviors. For temporal scales less than 84 hours, time development of earthquake radiated energy activity follows an algebraic arrangement consistent with estimates from the theory of nonequilibrium phase transitions. There are no characteristic scales for probability distributions of sizes and lifetimes of the activity bursts in the scaling region. The power-law exponents describing the probability distributions suggest that the main energy dissipation takes place due to largest bursts of activity, such as major earthquakes, as opposed to smaller activations which contribute less significantly though they have greater relative occurrence. The results obtained provide statistical evidence that earthquake energy dissipation mechanisms are essentially “scale-free”, displaying statistical and dynamical self-similarity. Our results provide some evidence that earthquake radiated energy and directed percolation belong to a similar universality class.

## 1 Introduction

Earthquakes represent an area of research with important theoretical and practical implications. In terms of basic human wellbeing, earthquakes are natural hazards with devastating consequences. As natural events, they possess qualities in common with other areas of scientific research and, as such, their universal qualities offer the tantalizing suggestion that with further research their shattering social and economic costs might be reduced.

A predominantly empirical approach is typically applied to energy dissipation and associated earthquake dynamics. Earthquakes are generally characterized by the well-known Gutenberg-Richter and Omori laws. These power-laws are viewed as the product of multiscale interactions and are themselves scale-invariant and unaffected by energy or time scales. But while these laws appear indifferent to energy or time scales earthquakes sometimes do exhibit characteristic energy scales.

An earthquake involves energy release in the form of seismic waves, with dynamics exhibiting intermittent temporal patterns where periods of high activity are separated by periods of relative quiet. Rather than a smooth path, earthquake dynamics follow an avalanche or punctuated type development reminding one of self-organized critical systems [1].

Over the past few decades research has begun to explore the possibility of seismicity being in a self-organized critical state [1–6]. These studies show how the earthquake energy release distribution (seism energy or avalanche size) follows a power law distribution, and how spatial distributions (of avalanches or the seism magnitude) shows (multi)fractal structure.

In this paper we propose to study ensemble-averaged statistical properties of earthquakes in Chile. Since we do not have detailed knowledge about underlying dynamics, it is important to attempt to explain the ensemble averaged arrangement of correlations to extract information of the dynamical features of a time series. In general when a nonlinear system has many sources of spatially dispersed instability it cannot be wholly characterized in deterministic terms. That is why a statistical analysis is necessary. Applicable statistical-physical methods of analysis allow one to extract a great deal of information about system dynamics found in multiscale correlations of non-Gaussian random variables [7]. Consequently, we frame the following working hypothesis: there exists a correlation, at least at the statistical level, between any two successive events. It does not matter how distant they are. In other words, one earthquake can trigger the next one over 1000 km away [8], and system correlation length can be divergently large. These factors suggests a similarity to critical phenomena.

<sup>a</sup> e-mail: denisse.pasten.g@gmail.com

Using this approach we seek to probe earthquake data to answer the following questions: Do seismic disturbances of various sizes exhibit a distinctive temporal signature? In terms of overall energy dissipation what are the relative contributions of large- and small-scale earthquakes? If there is a characteristic scale does this suggest the dominance of a specific dissipation mechanism?

Our work finds motivation in the above questions, which point to a few interesting and novel results regarding the temporal dynamics of earthquake energy radiation and dissipation. Various earthquake studies frequently demonstrate robust power-law statistical relations. We explore whether these are consistent with the dynamics of nonequilibrium systems undergoing transitions between several metastable states. Given that stress buildup is released within minutes, even seconds, we have an intuitive expectation that earthquakes, as a slowly driven threshold phenomenon, might exhibit such metastable, critical behavior. If such is the case it may suggest that the observed seismic activity bursts are not dominated by characteristic space, time, or energy scales; and so the energy dissipation mechanisms associated with earthquakes are essentially “scale-free”.

We already know the Omori and Gutenberg-Richter scalings hold for both energy and timing data. However, not all power law behavior is necessarily an effect of dynamical self-organization into a critical stationary state [9,10]. In this paper we wish to go beyond the well-known scaling behaviors and explore the question of whether earthquakes fit the hypothesis of an avalanching critical system. We propose to do this by defining and finding a set of new power law exponents explicitly predicted for critical avalanching systems.

## 2 Statistical theory

When equilibrium systems display critical behavior the most common characterization is via long-range correlations propagating through the system. This is usually realized by the fine-tuning of a control parameter [11]. What this demonstrates is that many systems, near their critical points, tend to produce long-range and scale-free correlations having universal statistical properties. The system in thermodynamic equilibrium, and system phase transitions, is the most familiar setting for discussion of critical system reconfigurations.

However, nonequilibrium situations such as the onset of fluid convection, also exhibit critical reconfigurations. Similarly, models of dynamics in markets [12], epidemics [13,14], space weather [15–19] and city traffic [20–22] are other respectable examples, and references above suggest the earthquakes follow a similar universality.

The nascent theory of nonequilibrium critical systems offers an explanation for scale-invariant dynamics in systems both driven and distorted. Critical behavior is, as mentioned above, often associated with fine tuning of one or more system parameters. Systems in a so-called self-organized critical (SOC) state exhibit scale-free correla-

tions, correlations usually accompanying criticality, giving the appearance of arising spontaneously. That is why it can be a frustrating exercise to search for a specific trigger that initiates the explosive system reconfiguration – there is often simply no unambiguously and unique trigger [23]. For example, if a system is in a SOC state it will be barely stable and far from equilibrium. Yet it will reliably return to the critical state again and again, thus responding resiliently to driving.

We note that a mere demonstration of scale-invariance at a point in parameter space is insufficient to elucidate the behavior of nonequilibrium natural systems. Furthermore, it does not directly offer any explanation of how to maintain the system at, or close to, the critical point. In the language of earthquake dynamics, the existence of power law behavior (e.g. Omori or Gutenberg-Richter) is not sufficient to guarantee that the dynamics are consistent with the statistics of a non-equilibrium critical avalanching system.

To explore such issues we will use recently developed frameworks [24,25] to describe dynamics of critical reconfigurations – the so-called avalanches [26] – taking place in a general class of nonlinear dynamical systems with coupled degrees of freedom. We will define  $N(\tau)$  as the average number of avalanche sites which are active. This is the same as the average excitation area in the continuum limit. Here we define the parameter  $\tau$  as the temporal interval each initiation of an avalanche. The nonequilibrium models mentioned above, for delay times less than the time-scale introduced by finite-size effects, predict that close to the critical point, the number of avalanche sites follows a power law scaling as follows  $N \propto \tau^\eta$ . If we define  $P_S(\tau)$  as the probability of an avalanche surviving by this time, then theory also predicts a power law scaling:  $P_S \propto \tau^{-\delta}$ . Two power law exponents  $\eta$  and  $\delta$  are introduced, called spreading-exponents [25]. The avalanche size  $S$  is the total number of active sites participating in the system rearrangement. The avalanche lifetime is represented by  $T$ . For SOC, which is a nonequilibrium critical state, there is a strong connection between avalanche lifetime and size. Following the definition of  $\delta$  and  $\eta$ , one can demonstrate how there must exist a scaling relationship for the average number of active sites in surviving runs which participated in producing avalanches with  $T > \tau$ . The scaling is on the order of  $\tau^{\delta+\eta}$ . Further, upon creating the time integral of this quantity to compute the characteristic size  $S$  of the event, we realize  $S \sim T^{1+\delta+\eta}$  (details are found in [25]). Such scaling relations comprise a central role in the statistical analysis of nonequilibrium critical systems [27–29].

We will see below, that the distributions for size and lifetime for this system follow power law distributions, and these two quantities are related through a power law relation. Furthermore, it is extremely important that these three power law indices satisfy the scaling relation (criticality relation), in a manner similar to what occurs in traditional theories of equilibrium phase transitions. Of course, in our case the system is clearly in a driven non-equilibrium state (by the subduction plate), so that in principle we cannot use traditional equilibrium

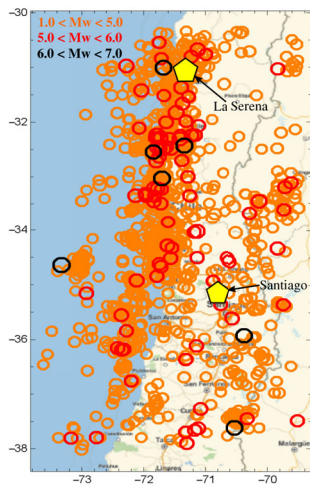


**Fig. 1.** Map of the central zone of Chile, with the seismic events with magnitudes greater than  $M_w = 1.6$ .

theory, and must resort to the analysis described in this manuscript. It is important to note that to have a non-equilibrium system at criticality; it is insufficient to show that we have power law distributions for size or duration, but that they should be related in a manner to satisfy the critical scaling relation.

In this paper we wish to examine the extent to which the avalanches of nonequilibrium statistical physics, mentioned above, can be related to bursts of seismic activity in the crust and mantle of the earth. In pursuit of this objective, we here demonstrate the time-series based version of spreading exponent studies [30] where bursts of seismic activity are treated as physical indicators of spatiotemporal spreading dynamics.

### 3 Data and analysis method

The data used for this paper was measured by the Chilean Servicio Sismológico Nacional (National Seismologic Service). They were recorded from October 2000 to January 2007 and comprise in excess of 17 000 seismic events of magnitude above 1.6. All data were recorded between longitudes  $69.5^\circ$  W and  $73.9^\circ$  W and latitudes between  $29.0^\circ$  S and  $35.5^\circ$  S. The data fall within a volume having dimensions  $L_z = 300$  km in depth,  $L_{NS} = 730$  km long in the North-South direction, and  $L_{EW} = 500$  km in the East-West direction. The zone studied is showed in Figure 1.

From these data we have the hypocenter (the 3D point of the seismic event), the time of seismicity, and the Richter or local magnitude  $M_L$  [31], which is directly related to the energy release and to the amplitude of the seismic event:

$$M_L = \log_{10}(A) - \log_{10}(A_0)\delta_0.$$

In this equation  $\delta_0$  is the distance between the observation location and epicenter,  $A$  is the amplitude of the  $S$ -waves measured 600 km from the epicenter, and  $A_0$  is a standard

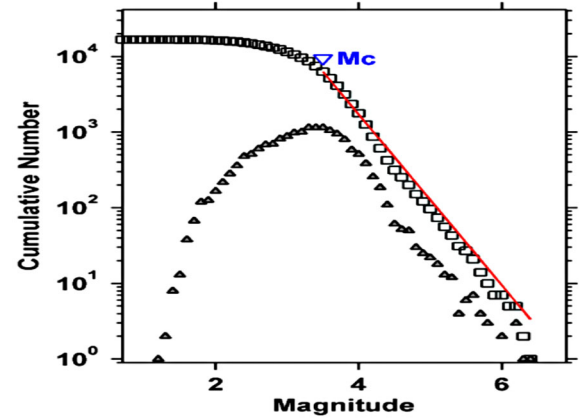


**Fig. 2.** Frequency-magnitude distribution for our earthquake catalogue. The red curve fits the cumulative distribution function to the point of maximum curvature.

value, depending on the temporal interval between  $P$ - and  $S$ -wave observation at the recording station.

We include a preliminary completeness analysis of our dataset. Following [32] we define the completeness magnitude  $M_c$  as the lowest magnitude at which all of the earthquakes in a space-time volume are detected. The magnitude where the lower end of the distribution of frequency versus magnitude leaves the Gutenberg-Richter law is taken as an estimate of  $M_c$ . We use the method of [33] in which  $M_c$  is estimated by fitting a Gutenberg-Richter model to the observed frequency-magnitude distribution. The expected relationship can be written as:

$$\log_{10} N = a - b(M - M_c).$$

Here  $N$  is the number of events with a magnitude larger than or equal to  $M$ ,  $a$  is the earthquake productivity, and  $b$  is related to the relative distribution of large and small earthquakes [34].

The fit is computed using a maximum curvature method as explained by [35]. In Figure 2 we show the results of this preliminary analysis.

Our best fit yields  $M_c = 3.4$ ,  $b = 1.13 \pm 0.01$ , and  $a = 7.75$ .

Since we wish to examine energy dissipation, the earthquake magnitudes must be convolved to seismic radiated energy:

$$E = 10^{4.8+1.5M_L},$$

where  $E$  is the radiated energy in joules [36]. Radiated energy is a dynamic measure of earthquake size that depends on the details of the rupture process. For instance, when there is slow slip on a fault, perhaps only a small amount of energy is radiated, yet this may have the same Richter magnitude in a felt earthquake which actually radiates far more energy.

Figure 3 shows the raw, unsmoothed radiated energy data. Note that these data, covering over seven orders of magnitude in energy, show evidence of strong intermittency, and have a multifractal nature [37–39]. Given

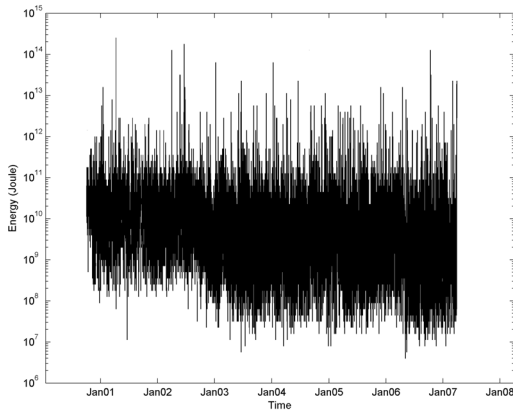


**Fig. 3.** Radiated energy for 2001 through 2007, with a strong intermittency.

that earthquake magnitudes, from which the radiated energy curve is calculated, are often like point processes in a given geographic region, there may be periods where radiated energy is below the measurement threshold so that there are only apparent intermittent spikes in energy above a zero threshold. Since the original data set considers seismic magnitudes only above 1.6, any lower magnitude tremors contribute zero to energy budgets as they are effectively ignored. In addition, each earthquake magnitude is given at a particular instant, whereas in reality the radiated energy profile is spread out, rather than a delta function. Since this is unrealistic, and since the effect is to have long gaps where there is no radiated energy reflected in our raw data, we convolve the time series of earthquake magnitudes to create a modified radiated energy profile.

First we produce a time series of radiated energy on a uniform grid. This mitigates the effects of long gaps with no seismic activity. Next we smooth the radiated energy data using a running average filter. Smoothing the radiated energy data using a running average filter avoids the problem of the most energetic seismic events destroying information contained in lower energy events found in an averaging box. Specifically we use a second degree polynomial model to perform a local regression with weighted linear least-squares. This reduces the impulsive nature of the raw data by flattening the raw energy profile.

We create the final cumulative radiated energy time series by summing the energy within a box of length 1 week, then moving the box through the data with a step size of 1 min.

We selected this temporal cadence and box size because the minimum gap between recorded seismic events is on the order of a minute and the maximum time interval between seismic activity above the minimum threshold is 2.2 days. We experimented to see the results of our analysis with different box sizes, and found little difference within the experimental uncertainty.

The smoothing reduces the dominance of local seismic events that are orders above the average, and spread the

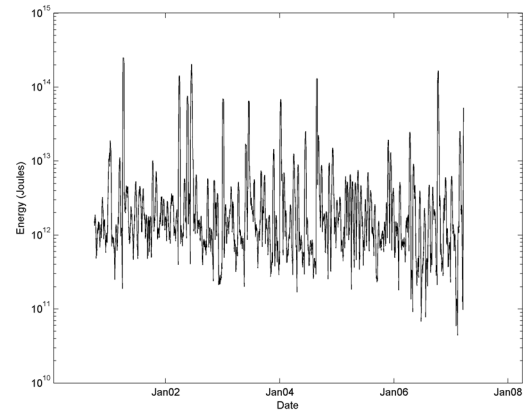


**Fig. 4.** Radiated energy profile.

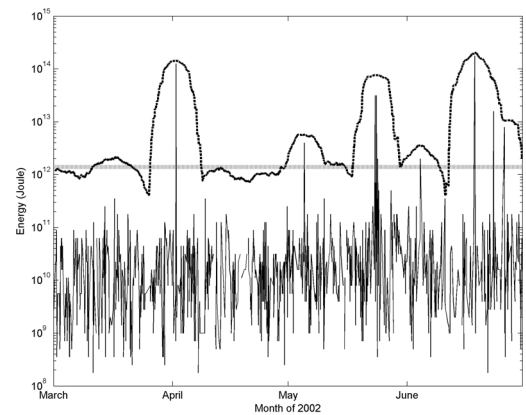


**Fig. 5.** Comparison of the raw point process radiated energy profile for March through June 2002, showing large intermittency, and the smoothed total radiated energy. The horizontal line shows the 50th percentile for the full data set shown in Figure 3.

energy of these events. This can be seen in Figure 4, which shows energy data. These data are less intermittent than the raw data of Figure 3. Figure 5 shows a comparison of the raw radiated energy profile and the original point process nature of the raw data. The raw radiated energy profile is highly intermittent compared to the modified radiated energy.

Note from this figure how the modified radiated energy profile smooths the data but retains the continued effect of the dominant seismic event within a given box which, though still evident, no longer makes irrelevant the other seismic events within any given box. For instance, see around April 1, 2002, May 1, 2002, and just prior to June 1, 2002.

Now that we possess a reasonable measure of cumulative energy radiation, we can assess the extent of the seismic behavior that reflects critical behavior. If the energy perturbations are near a critical state, it should be possible to recover some, perhaps all, power-law relations introduced in the previous section.

To do so we follow the methodology of [30] and decompose the radiated energy data into series of activity bursts. We define an activity burst ( $AB$ ) to be a transient increase of the seismic radiated energy, from the time series shown in Figures 4 and 5. Such an  $AB$  is flagged if the data exceed a specified constant threshold. We define the waiting-time as the time interval between two such bursts of activity. If a system is SOC-like there can be a broad range of thresholds where gradients of the power-law portion of the burst lifetime distribution are constant [40].

We define as the lifetime  $T$  for each  $AB$  the temporal interval during which the data exceeds the threshold. In addition we compute the  $AB$  size,  $S = \int_{\{T\}} (E_{\text{rad}}(t) - L) dt$ , where  $L$  is the selected threshold.  $E_{\text{rad}}$  is the cumulative radiated energy data, reflecting the dissipation of stress within Earth's crust.

We follow definitions of  $S$  and  $T$  that match energy-based estimates of sizes and lifetimes of critical avalanches in “running, continuously driven” SOC models [41]. This is relevant, as the time series of individual earthquakes does not contain specific information on either size or duration of a given event (which can be thought of as a single avalanche), and thus another criterion needs to be established to estimate both  $S$  and  $T$ . Regarding the size estimate, in some sandpile models the number  $N$  of active elements is commonly proportional to the energy dissipated, thus we use an analogous reasoning for the cumulative radiated seismic energy to define an  $N^*$  scaling in much the same manner as  $N$ ;  $N^* = \langle E_{\text{rad}}(t_1 + \tau) - L \rangle$ . Thus, the size of the event is estimated from the energy released.

The estimation of the duration of the avalanche is less straightforward. One reason is the fact that the earthquake time series does not have information on the duration of the earthquakes. Another reason is that a single seism can trigger others, making the very definition of “event” non trivial. But, as suggested in [41], a state with interacting avalanches can be thought of as the aftershock regime following a main shock. This is what the smoothing process described above intends to represent. Rather than considering an earthquake as a single event, by smoothing the time series we can define an event as a number of seisms. For seisms with a large separation in time, this is equivalent to considering each event as a single avalanche, as expected. But if many seisms are very close in time (such as in aftershocks or seismic swarms), the smoothing process allows them to be regarded as a single event of energy release. Hence, the notion of the duration of an event becomes clear when considering it as a sequence of seisms. Once the smoothed events are found, the prospect an  $AB$  lasts beyond a certain time interval is termed the survival probability,  $P_S(\tau) = n(\tau)/m$ , where  $n$  is the number of  $AB$ s with  $T > \tau$  and  $m$  is the total number of  $AB$ s.

## 4 Results and discussion

The top panel of Figure 6 shows plots of  $N^*(\tau)$  for cumulative radiated seismic energy and its bottom panel shows the associated plots for the survival probabilities

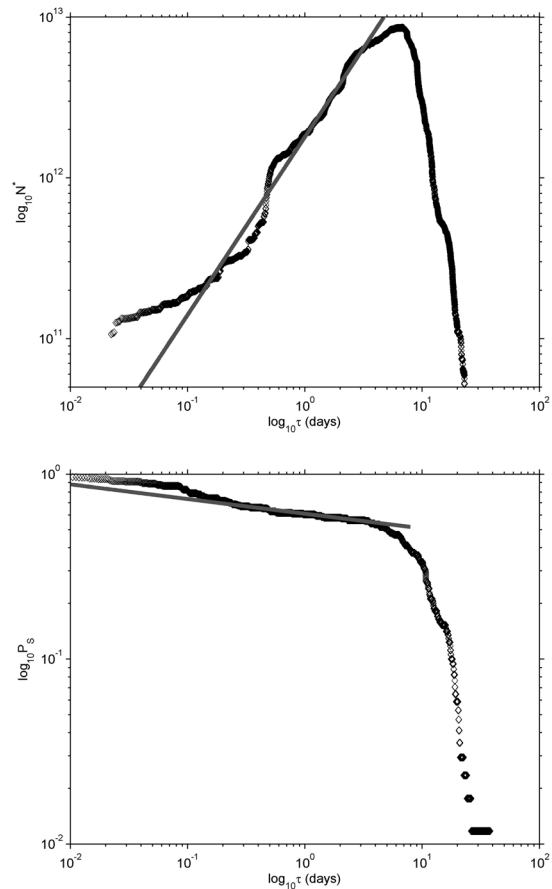


**Fig. 6.** Top panel:  $N^*$  as a function of lifetime  $\tau$ . Bottom panel: survival probability  $P_S$  as a function of lifetime  $\tau$ .

$P_S(\tau)$ . In these figures we show results for the threshold of  $L = 1.39 \times 10^{12}$  J which corresponds to the 50th percentile for our data signal; this corresponds to values significantly above the associated completeness magnitude determined previously. We find simultaneous power-law fits over a broad range of thresholds  $L$  for cumulative radiated seismic energy, up to the 90th percentile. There is some divergence for the power law fits for the smallest lifetimes, and a strong break in the average number of activity bursts past periods of 3 days. We therefore attempt to fit a power law over the interval  $\tau < 3.5$  days. Fitting of power laws is difficult and an extensive literature demonstrates a preference for maximum-likelihood methods [42], which we follow as well. We use the robust Levenberg-Marquardt algorithm for nonlinear least squares [43], to estimate best-fit critical scaling exponents,  $\eta = 1.11 \pm 0.01$  and  $\delta = 0.079 \pm 0.001$ .

In the event they exist it is possible to relate theoretical dynamic critical exponents with avalanche scaling exponents. The latter are estimated via probability distributions of avalanche sizes and lifetimes. We fit avalanche and lifetime distributions by power laws with exponential cutoffs, namely  $P_S \propto S^{-\eta} \exp(-S/S_C)$  and  $P(T) \propto T^{-\delta} \exp(-T/T_C)$ . The exponential cutoffs account for deviation from self-similar statistics at the largest scales

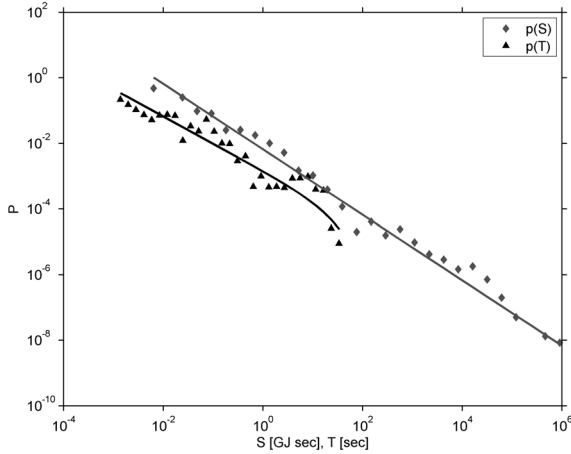


**Fig. 7.** Avalanche probability distributions  $P(S)$  (grey diamonds) and  $P(T)$  (black triangles) for the threshold of  $L = 1.39 \times 10^{12}$  J.

**Table 1.** Avalanche scaling exponents from the lifetime and avalanche size probability distributions for various  $AB$  thresholds.

| Threshold                     | $t_S$           | $t_T$           |
|-------------------------------|-----------------|-----------------|
| 90 ( $6.93 \times 10^{12}$ J) | $1.00 \pm 0.04$ | $0.81 \pm 0.08$ |
| 75 ( $3.03 \times 10^{12}$ J) | $0.92 \pm 0.02$ | $0.82 \pm 0.06$ |
| 50 ( $1.39 \times 10^{12}$ J) | $0.96 \pm 0.02$ | $0.81 \pm 0.05$ |
| 25 ( $0.78 \times 10^{12}$ J) | $1.00 \pm 0.03$ | $0.94 \pm 0.05$ |
| 10 ( $0.45 \times 10^{12}$ J) | $0.99 \pm 0.03$ | $0.93 \pm 0.04$ |

resulting from the paucity of such seismic events. In Figure 7 we plot these distributions for the threshold at the 50th percentile.

To demonstrate the robustness of the power law exponents, irrespective of  $L$ -threshold used, Table 1 presents the fitting parameters calculated from the probability distributions for multiple thresholds. There is reasonable agreement except for at and below the 25th percentile for  $t_T$ . This deviation may exist because there are simply insufficient avalanches at this threshold to measure reasonable statistics.

Consider now the overall earthquake radiated energy dissipation. Our results present the opportunity to contrast and compare the relative importance of small and large  $AB$ s. Given the scaling ansatz for  $p(S)$  previously introduced the rate of total energy release by the ensemble of bursts scales like:

$$E_{\text{tot}} \sim \int_{S_0}^{S_C} S p(S) dS \sim \frac{S^{2-t_S}}{2-t_S} \Big|_{S_0}^{S_C}, \quad t_S \neq 2, \quad (1)$$

where  $S_0 \ll S_C$  is the tiniest burst size. Large bursts dictate the release of energy if  $t_S < 2$ , and small  $AB$ s dominate the energetics when  $t_S > 2$ . We find  $t_S$  much below 2, which suggests that large  $AB$ s are most important in the dissipation of earthquake total energy.

Let us now attempt to relate the avalanche exponents  $t_S$  and  $t_T$ . First note that conservation of probability

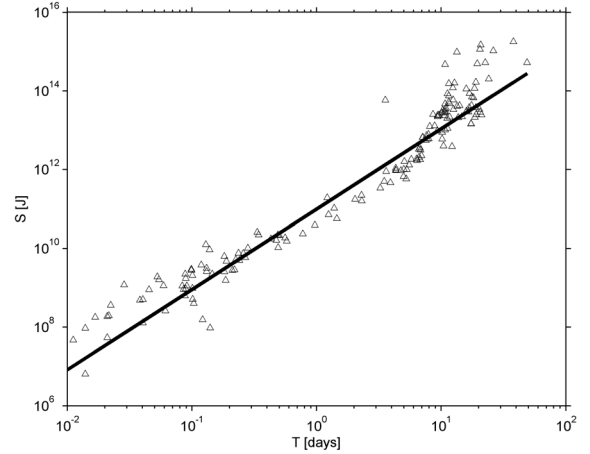


**Fig. 8.** Burst size  $S$  as a function of lifetime  $T$ .

gives  $p(S)dS \sim p(T)dT$  and then apply the scaling law  $S \sim T^{1+\delta+\eta}$  which was derived previously. Then, over the power-law regions, we find  $t_T = (1 + \delta + \eta)(t_S - 1) + 1$ . Because  $\delta$  is the survival probability exponent, it should relate directly to the cumulative avalanche lifetime probability distribution; it equals the power-law slope  $t_T - 1$ . This produces  $t_T = (\eta[t_S - 1] + 1)/(2 - t_S)$ . The scaling relation we find matches the analysis of spreading and avalanche exponents first introduced by [25]. They found that  $t_S = (\eta + 2\delta + 1)/(\eta + \delta + 1)$ . This expression contracts to our formula following the substitution  $\delta = t_T - 1$ . The theoretical value then, calculated from  $N^*(\tau)$ , is  $t_T = 1.08 \pm 0.01$  which compares favourably with the values calculated from  $p(T)$ , viz.  $t_T = 1.02 \pm 0.09$ .

The relation  $t_S = (\eta + 2\delta + 1)/(\eta + \delta + 1)$  works fairly well in the case of the earthquake radiated energy for the area of Chile we have examined: the predicted value is  $t_S = 1.03 \pm 0.01$ , which is close to the value measured directly via  $p(S)$ , viz.  $t_S = 1.00 \pm 0.05$  (the two estimates are statistically indistinguishable at the confidence test level  $p = 0.95$ ).

Figure 8 shows avalanche size versus lifetime. The largest earthquake seisms broaden the range of sizes for the largest lifetimes. The best-fit critical exponent calculated from the local slope was  $2.04 \pm 0.16$ . In critical avalanching systems, the lifetimes and sizes are related by  $S \propto T^{1+\eta+\delta}$ . Our results show the strong connection between the experimental theoretical value between avalanche lifetime and size  $(1 + \eta + \delta) = 2.29 \pm 0.02$ .

In Table 2 we summarize the results, giving scaling exponents measured directly from power laws produced by the seismic processes, and comparing these to theoretical predictions calculated from  $\eta$  and  $\delta$  values. These latter values we derive from  $N^*(\tau)$ , the average number of active avalanche sites, and the survival probabilities  $P_S(\tau)$ .

It is interesting to observe the match between measured and theoretical values of the scaling exponents  $t_S$  and  $t_T$  as shown in Table 2, in view of the assumptions involved in the definition of activity burst as described in Section 3. In reference [30] the same method was applied but unlike the earthquake series, the time series used

**Table 2.** Compilation of the theoretical values for scaling exponents, calculated from  $\eta$  and  $\delta$ , and the equivalent experimental measurements from actual distributions.

| Exponent            | Measurement       | Theory          |
|---------------------|-------------------|-----------------|
| $\eta$              | $1.11 \pm 0.01$   | –               |
| $\delta$            | $0.079 \pm 0.001$ | –               |
| $t_S$               | $1.00 \pm 0.05$   | $1.03 \pm 0.01$ |
| $t_T$               | $1.02 \pm 0.09$   | $1.08 \pm 0.01$ |
| $\eta + \delta + 1$ | $2.04 \pm 0.16$   | $2.19 \pm 0.02$ |

in [30] is a continuous record of space science activity index data, and thus the duration of an event has a direct meaning. Here, only data for individual seisms are available. However, seismic energy is not necessarily released in single events, such as when aftershocks or seismic swarms occur, and thus activity bursts are defined in terms of a longer time scale by means of a smoothing process, which allows several, close-in-time events, to contribute to a single burst. There are several ways in which the process could be improved (tuning the window size for smoothing, or the threshold to define a burst), so we regard this approach as a first approximation to the problem, but it is encouraging that our method yields results consistent with SOC behavior for seismicity, beyond the well known Omori and Gutenberg-Richter laws.

## 5 Conclusion

We have found two different echelons of results. The first is observational evidence of broad-range scaling in earthquake radiated energy dynamics between October 2000 and January 2007, for latitudes  $29.0^\circ$  S to  $35.5^\circ$  S, and between longitudes  $69.5^\circ$  W and  $73.9^\circ$  W.

Our analysis adds a helpful piece of information to existing portraits of earthquake energy dissipation by uncovering its multiscale nonlinearity. We have shown the absence of any time scales where the earthquake radiated energy response is linear. Our results go beyond standard power-law behaviors like the Omori and Gutenberg-Richter laws, and may serve as an additional validation tool for models of earthquake energy dissipation in terms of their ability to represent correctly effects of cross-scale coupling [44].

The second level of results, so far less concrete, shows how earthquake energy dissipation, and attendant multiscale dynamics, results from cooperative behavior ruled by a specific statistical principle. We associate such dynamical behavior with nonlinear interactions of spatially extended degrees of freedom (e.g. multiscale fracture and stress regimes in rock) that maintain the system in the region of a global critical point. Such an interpretation, while supported by the achieved statistics, is far from final. On the basis of simulation results for nonlinear critical models [45], our evidence points to the idea that earthquake radiated energy comes from a geophysical mechanism that connects a one-dimensional mass and/or energy transport realized in a medium of two-dimensions. This matches ex-

pectations for the fracture process, or even dynamics of large-scale fault slippage [46,47].

In summary, temporal development of bursts of radiated earthquake energy follows statistical forms matching predictions from theories of nonequilibrium phase transitions. Our results provide direct evidence for dynamical and statistical self-similarity in earthquake energy dissipation and signal its possible critical behavior. The existence of a dynamic critical power-law exponent of burst size distribution suggests that the main energy dissipation is associated with large *ABs* such as major quakes. Smaller activations contribute less despite their larger relative occurrence. This is consistent with the well-known energy dissipation laws. Based on the  $t_S$  value obtained, the rate of total seismic energy radiated scales as  $S_C^{-t_S+1} \sim S_C^{0.9}$  meaning it is governed by the upper cutoff scale, which diverges in the limit  $S_C \rightarrow \infty$ . However, we find that we can describe the  $P(S)$  distribution by a single power-law exponent. This suggests that both small- and large-scale *ABs* can be a indicator of emergent behavior allied with intensive cross-scale coupling of multiple intrinsic dissipation mechanisms.

These results begin to paint a coherent portrait of critical fluctuations in earthquakes. Of course, the mere existence of uncomplicated algebraic relations between multiple kinds of scaling exponents is not a definitive indication of critical systems. Scaling relations arise for any fractal stochastic process. But the form of the scaling can vary quite a bit depending on the underlying physics. For example, in fractional Brownian motion (fBm), multifractional Brownian motion (mfBm) [48], or other processes [49]. Peng et al. [50] used a time-varying threshold in fBm to determine that  $t_S = 2/(1 - H)$  and  $t_T = 2 - H$ , and so  $t_T = 3 - (2/t_S)$ . This implies that  $t_T$  can be defined uniquely via the value of the exponent  $t_S$  irrespective of the Hurst exponent  $H$  which describes the time series correlation structure. Therefore, fBm scaling is quite different from that found in some critical avalanching systems, and in the dynamics of earthquake radiated energy.

We do not wish to overstate the consistency of the earthquake energy dissipation dynamics with the scaling relations predicted for a specific class of critical models with absorbing configurations (see e.g. [24,25,45]). Hinrichsen's review [51] notes the existence of these absorbing states. He calls these, "a highly idealized requirement that is difficult to realize experimentally". But we note that it has recently been achieved [52,53]. It remains open whether it is possible to treat earthquake dynamical states as absorbing configurations. Our analysis of seismic dynamic critical scaling exponents supports the confirmatory reply.

This material is based upon work supported by the National Science Foundation under Grant No. AGS-1104364. We also thank the support of Fondecyt Grants 1150718, 1130273, and 1161711. Earthquake data are courtesy of the Chilean Servicio Sismológico Nacional (National Seismologic Service). D.P. thanks Advanced Mining Technology Center. We thank the support of CEDENNA and the US AFOSR Grant FA9550-16-1-0384.

## Author contribution statement

James Wanliss did the main analysis and was involved in scientific discussions for Sections 1, 2, 3, 4 and 5. Víctor Muñoz was involved in the redaction of the whole text, and scientific discussions for Sections 1, 2, 3, 4 and 5. Denisse Pastén obtained the data from the National Seismological Center in Chile and she was involved in scientific discussions for Sections 1, 3, 4 and 5. Benjamín Toledo had part in scientific discussions for Section 4. Alejandro Valdivia was involved in the redaction of the text and scientific discussions for Sections 1, 2, 3, 4 and 5.

## References

1. A. Sornette, D. Sornette, *Europhys. Lett.* **9**, 197 (1989)
2. D. Pastén, V. Muñoz, A. Cisternas, J. Rogan, J.A. Valdivia, *Phys. Rev. E* **84**, 066123 (2011)
3. J.X. de Carvalho, C. Prado, *Phys. Rev. Lett.* **84**, 4006 (2000)
4. T. Chelidze, T. Matcharashvili, *Tectonophysics* **431**, 49 (2007)
5. K. Ito, M. Matsuzaki, *J. Geophys. Res. B* **95**, 2156 (1989)
6. P. Bak, C. Tang, *J. Geophys. Res. B* **94**, 15635 (1989)
7. R. Chicheportiche, A. Chakraborti, *Phys. Rev. E* **89**, 042117 (2014)
8. D.W. Steeples, D.D. Steeples, *Bull. Seismol. Soc. Am.* **86**, 921 (1996)
9. N.W. Watkins, *Nonlinear Proc. Geophys.* **9**, 389 (2002)
10. N.W. Watkins, D. Credington, R. Sanchez, S.J. Rosenberg, S. Chapman, *Phys. Rev. E* **79**, 041124 (2009)
11. H.E. Stanley, *Rev. Mod. Phys.* **71**, S538 (1999)
12. N. Lammoglia, V. Muñoz, J. Rogan, B. Toledo, R. Zarama, J.A. Valdivia, *Phys. Rev. E* **78**, 047103 (2008)
13. J.L. Cardy, P. Grassberger, *J. Phys. A* **18**, L267 (1985)
14. H.K. Janssen, *Z. Phys. B* **58**, 311 (1985)
15. A.J. Klimas, J.A. Valdivia, D. Vassiliadis, D.N. Baker, M. Hesse, J. Takalo, *J. Geophys. Res.* **105**, 18765 (2000)
16. M.I. Sitnov, A.S. Sharma, K. Papadopoulos, D. Vassiliadis, J.A. Valdivia, A.J. Klimas, *J. Geophys. Res. A* **105**, 12955 (2000)
17. J.A. Valdivia, J. Rogan, V. Muñoz, B. Toledo, *Space Sci. Rev.* **122**, 313 (2006)
18. J.A. Valdivia, J. Rogan, V. Muñoz, B. Toledo, M. Stepanova, *Adv. Space Res.* **51**, 1934 (2013)
19. M. Domínguez, V. Muñoz, J.A. Valdivia, *J. Geophys. Res.* **119**, 3585 (2014)
20. B.A. Toledo, V. Muñoz, J. Rogan, C. Tenreiro, J.A. Valdivia, *Phys. Rev. E* **70**, 016107 (2004)
21. J. Villalobos, B.A. Toledo, D. Pastén, V. Muñoz, J. Rogan, R. Zarama, N. Lammoglia, J.A. Valdivia, *Chaos* **20**, 013109 (2010)
22. B. Toledo, M.A.F. Sanjuan, V. Muñoz, J. Rogan, J.A. Valdivia, *Commun. Nonlinear Sci. Numer. Simul.* **18**, 81 (2013)
23. J.A. Wanliss, *J. Geophys. Res. A* **110**, 10544 (2005)
24. R. Dickman, *Phys. Rev. E* **53**, 2223 (1996)
25. M.A. Muñoz, R. Dickman, R. Pastor-Satorras, A. Vespignani, S. Zapperi, *Sandpiles and Absorbing-State Phase Transitions: Recent Results and Open Problems*, in *Modeling Complex Systems: Sixth Granada Lectures on Computational Physics*, edited by P.L. Garrido, J. Marro (2001), Vol. 574, p. 102
26. P. Bak, C. Tang, K. Wiesenfeld, *Phys. Rev. A* **38**, 364 (1988)
27. M. Paczuski, S. Maslov, P. Bak, *Phys. Rev. E* **53**, 414 (1996)
28. J. Marro, R. Dickman, *Nonequilibrium Phase Transitions in Lattice Models* (Cambridge University Press, Cambridge, 1999)
29. R. Dickman, M.A. Muñoz, A. Vespignani, S. Zapperi, *Braz. J. Phys.* **30**, 27 (2002)
30. J. Wanliss, V. Uritsky, *J. Geophys. Res.* **115**, A03215 (2010)
31. C.F. Richter, *Elementary Seismology* (W. H. Freeman & Co., Princeton, USA, 1958)
32. P.A. Rydelek, I.S. Sacks, *Nature* **337**, 251 (1989)
33. F.R. Zuniga, M. Wyss, *Bull. Seismol. Soc. Am.* **85**, 1858 (1995)
34. B. Gutenberg, C.F. Richter, *Bull. Seismol. Soc. Am.* **34**, 185 (1944)
35. S. Wiemer, M. Wyss, *Bull. Seismol. Soc. Am.* **90**, 859 (2000)
36. M. Bath, *Phys. Chem. Earth* **7**, 115 (1966)
37. D. Pastén, D. Comte, *J. Seismol.* **18**, 707 (2014)
38. P. Diodati, F. Marchesoni, S. Piazza, *Phys. Rev. Lett.* **67**, 2239 (1991)
39. P. Diodati, P. Bak, F. Marchesoni, *Earth Planet. Sci. Lett.* **182**, 253 (2000)
40. J. Wanliss, J. Weygand, *Geophys. Res. Lett.* **34**, 04107 (2007)
41. T. Hwa, M. Kardar, *Phys. Rev. A* **45**, 7002 (1992)
42. A. Deluca, P. Puig, A. Corra, Testing universality and goodness-of-fit test of power-law distributions, in *Extended Abstracts Spring 2013, Trends in Mathematics*, edited by A. Corral, A. Deluca, F. Font-Clos, P. Guerrero, A. Korobeinikov, F. Massucci (Birkhäuser, Cham, 2014), Vol. 2, pp. 13–18
43. G.A.F. Seber, C.J. Wild, *Nonlinear Regression*, Wiley Series in Probability and Statistics (Wiley, 2005)
44. P. Bhattacharya, B.K. Chakraborti, Kamal, A fractal model of earthquake occurrence: theory, simulations and comparisons with the aftershock data, in *Continuum Models and Discrete Systems Symposia (CMDS-12)*, Journal of Physics: Conference Series (2011), Vol. 319, p. 012004
45. M.A. Muñoz, R. Dickman, A. Vespignani, S. Zapperi, *Phys. Rev. E* **59**, 6175 (1999)
46. Y. Ben-Zion, J.R. Rice, *J. Geophys. Res. B* **102**, 17771 (1997)
47. S. Xu, Y. Ben-Zion, J.P. Ampuero, V. Lyakhovskiy, *Pure Appl. Geophys.* **172**, 1243 (2014)
48. J.A. Wanliss, K. Shiokawa, K. Yumoto, *Nonlinear Proc. Geophys.* **21**, 347 (2014)
49. V. Anh, Z.G. Yu, J. Wanliss, S. Watson, *Nonlinear Proc. Geophys.* **12**, 799 (2005)
50. C.K. Peng, S.V. Buldyrev, S. Havlin, M. Simons, H.E. Stanley, A.L. Goldberger, *Phys. Rev. E* **49**, 1685 (1994)
51. H. Hinrichsen, *Physica A* **369**, 1 (2006)
52. A.T. Kazumasa, M. Kuroda, H. Chaté, M. Sano, *Phys. Rev. E* **80**, 051116 (2009)
53. H. Hinrichsen, *Physics* **2**, 96 (2009)